# Norgestrel, a Progesterone Analogue, Promotes Significant Long-Term Neuroprotection of Cone Photoreceptors in a Mouse Model of Retinal Disease

Sarah L. Roche,[1] Oksana Kutsyr,[2] Nicolás Cuenca,[2] and Thomas G. Cotter[1]

[1]Cell Development and Disease Laboratory, Biochemistry Department, Biosciences Institute, University College Cork, Cork, Ireland
[2]Department of Physiology, Genetics and Microbiology, University of Alicante, San Vicente del Raspeig, Spain

Correspondence: Thomas G. Cotter, Cell Development and Disease Laboratory, Biochemistry Department, Biosciences Institute, University College Cork, Cork T12 YT20, Ireland;
t.cotter@ucc.ie.

Submitted: April 3, 2019
Accepted: June 25, 2019

Citation: Roche SL, Kutsyr O, Cuenca N, Cotter TG. Norgestrel, a progesterone analogue, promotes significant long-term neuroprotection of cone photoreceptors in a mouse model of retinal disease. *Invest Ophthalmol Vis Sci*. 2019;60:3221–3235. https://doi.org/10.1167/iovs.19-27246

**Purpose.** Retinitis pigmentosa (RP) refers to a group of inherited blinding retinal diseases, whereby the death of mutated rod photoreceptors is followed closely by the death of cone photoreceptors. Cone cell death can be hugely debilitating as color/daytime vision becomes impaired. Thus, treatments that are effective against cone cell death are urgently needed. Our research has been working toward development of a neuroprotective treatment for RP. We have previously demonstrated significant neuroprotective properties of norgestrel, a progesterone analogue, in the mouse retina. The current study further investigates the potential of norgestrel as a treatment for RP, with a focus on long-term preservation of cone photoreceptors.

**Methods.** Using the well-established rd10 mouse model of RP, we administered a norgestrel-supplemented diet at postnatal day (P)30, following widespread loss of rod photoreceptors and at the outset of cone degeneration. We subsequently assessed cone cell morphology and retinal function at P50, P60, and P80, using immunohistochemistry, electroretinograph recordings, and optomotor testing.

**Results.** While cone cell degeneration was widespread in the untreated rd10 retina, we observed profound preservation of cone photoreceptor morphology in the norgestrel-treated mice for at least 50 days, out to P80. This was demonstrated by up to 28-fold more cone arrestin-positive photoreceptors. This protection transpired to functional preservation at all ages.

**Conclusions.** This work presents norgestrel as an incredibly promising long-term neuroprotective compound for the treatment of RP. Crucially, norgestrel could be used in the mid-late stages of the disease to protect remaining cone cells and help preserve color/daytime vision.

Keywords: retinitis pigmentosa, cone photoreceptors, neuroprotection, progesterone, rd10

Retinitis pigmentosa (RP) is the most prevalent inherited retinal disease, affecting 2 million people worldwide. Mutations in over 60 genes have been implicated in RP that are expressed almost exclusively in rod photoreceptors,[1,2] and ultimately result in rod cell demise and reduced vision in low light (nyctalopia). During this stage, vision in bright light is largely unaffected as cone cells continue to function. Although rarely mutated, cone cells die as a consequence of the death of neighboring rod photoreceptors. This has detrimental effects on vision in daylight (achromatopsia). Hence, therapeutic approaches that promote cone cell survival in RP would be life-changing for those affected. It is vital that such therapeutic interventions be effective when administered during or following rod cell death, as rod cell death can go unnoticed for some time and accounts for up to 95% photoreceptor loss.[3]

Rods are a vital source of trophic support for cones throughout life.[4] Loss of trophic support from rods precedes an exposure to toxic reactive oxygen species (ROS), generated from the death of rods.[5,6] Hence, oxidative stress is a major contributory factor in the death of cone cells.[7] Starvation of nutrients, leading to a dysregulation of cellular metabolism, was demonstrated to drive cone cell death in RP.[8] As cone cells die, they release chemoattractants that mobilize and attract inflammatory cells, which can potentiate cone cell death.[9–11] Therefore, a loss of trophic support, nutrient deprivation, oxidative stress, and inflammation are all implicated in cone cell death in RP.

The widely studied rd10 mouse model harbors a point mutation in *pde6b*, which encodes for phosphodiesterase 6b,[12] an essential component of the rod phototransduction cascade. Mutations in *pde6b* are found in nonsyndromic cases of RP.[2,13] Retinal degeneration in the rd10 retina transpires as an initial, rapid loss of rod photoreceptors in the first 3 postnatal weeks, followed closely by a slower degeneration of cone cells into adulthood.[14–16]

Studies have shown that cone cell survival can be prolonged in animal models of retinal disease by combating processes such as trophic factor loss, nutrient deprivation, inflammation, and oxidative stress.[5,8,17–23] In 2011, we revealed the neuroprotective properties of norgestrel, a synthetic progestin (progesterone analogue), in the rd10 mouse[24] and since then in several models of retinal degeneration.[25–28] These studies involved administration of norgestrel prior to photoreceptor cell death and assessment of degeneration in the early stages. As

Table. List of Antibodies Used for Immunofluorescence and Western Blotting

| Antibody | Supplier | Catalogue No. | Host | Dilution |
|---|---|---|---|---|
| Cone arrestin | Merck Millipore | AB15282 | Rabbit polyclonal | IF 1:100 |
| Rhodopsin | Thermo Fisher Scientific | MS-1233 | Mouse monoclonal | IF 1:100 |
| Synaptophysin | Merck Millipore | MAB5258 | Mouse monoclonal | IF 1:500 |
| Iba1 | Wako | 019-19741 | Rabbit polyclonal | IF 1:500 |
| CD68 | AbD Serotec | MCA1957 | Rat monoclonal | IF 1:500 |
| GFAP | Dako | Z0334 | Rabbit monoclonal | IF 1:500<br>WB 1:1000 |
| Glutamine synthetase | Merck Millipore | MAB302 | Mouse monoclonal | IF 1:100<br>WB 1:1000 |
| Acrolein | Abcam | Ab37110 | Rabbit polyclonal | IF 1:500 |
| SOD1 | Abcam | Ab13498 | Rabbit polyclonal | WB 0.2 μg/mL |
| SOD2 | Abcam | Ab13533 | Rabbit polyclonal | WB 1:5000 |
| Catalase | Cell Signaling | 14097 | Rabbit monoclonal | WB 1:1000 |
| Glutathione reductase | Abcam | Ab16801 | Rabbit polyclonal | WB 1:2000 |
| Glutathione Peroxidase | Abcam | Ab22604 | Rabbit polyclonal | WB 1 μg/mL |
| Bcl-2 | Cell Signaling | 2870 | Rabbit monoclonal | WB 1:1000 |
| Bax | Cell Signaling | 2772 | Rabbit polyclonal | WB 1:1000 |
| Caspase 3 | Cell Signaling | 9662 | Rabbit polyclonal | WB 1:1000 |
| Caspase 9 | Cell Signaling | 9508 | Mouse monoclonal | WB 1:1000 |
| pAkt | Cell Signaling | 9271 | Rabbit polyclonal | WB 1:1000 |
| Akt | Cell Signaling | 9272 | Rabbit polyclonal | WB 1:1000 |
| mTOR | Cell Signaling | 5536 | Rabbit monoclonal | WB 1:1000 |
| TOR | Cell Signaling | 2983 | Rabbit monoclonal | WB 1:1000 |
| pERK1/2 | Cell Signaling | 9106 | Mouse monoclonal | IF 1:500<br>WB 1:2000 |
| pERK1/2 | Cell Signaling | 4376 | Rabbit monoclonal | IF 1:500 |
| ERK1/2 | Cell Signaling | 9102 | Rabbit polyclonal | WB 1:1000 |
| pMEK1/2 | Cell Signaling | 9154 | Rabbit monoclonal | WB 1:1000 |
| MEK1/2 | Cell Signaling | 8727 | Rabbit monoclonal | WB 1:1000 |

Supplier locations: Merck Millipore (Burlington, MA, USA); Wako (Richmond, VA, USA); AbD Serotec (Hercules, CA, USA), Dako (Santa Clara, CA, USA), Abcam (Cambridge, UK), Cell Signaling (Danvers, MA, USA), Thermo Fisher Scientific (Waltham, MA, USA). IF, immunofluorescence; WB, Western blotting.

mentioned earlier, therapeutic approaches that are effective in the later stages of the disease are needed. In the current study, we investigated the efficacy of norgestrel in protecting cone cells over long periods and in an already degenerating retina. This is essential to study, as cone and rod cell death differ greatly in terms of the rate and underlying cellular and molecular processes.[7,29,30] Therefore, we cannot assume that norgestrel's neuroprotective capacity is independent of the degenerative stage of the retina and the photoreceptor cell type undergoing cell death. We administered a norgestrel-supplemented diet to rd10 mice at postnatal day (P)30, when rod cell death is almost complete and cone cell degeneration is beginning. We subsequently assessed cone cell survival and function at P50, P60, and P80.

## Materials and Methods

### Mice

All animals were handled and maintained following the ARVO Statement for the Use of Animals in Ophthalmic and Vision Research (License AE19130). Experiments were approved by University College Cork Animal Experimentation Ethics Committee and were performed using both male and female C57BL/6 and homozygous rd10/rd10 mice (B6.CXBI-Pde6b$^{rd10}$/J). Mice were supplied by the Biological Services Unit, University College Cork and were humanely euthanized by cervical dislocation. Mice were exposed to a 12-hour light:12-hour dark cycle.

### Norgestrel-Supplemented Diet

Norgestrel-supplemented and control diets were manufactured by TestDiet (St. Louis, MO, USA). Norgestrel was added to the chow at a concentration of 0.05% (500 ppm). Rd10 mice were given a norgestrel-supplemented diet (TestDiet; LabDiet 9GWW, custom diet containing D(−) norgestrel; norgestrel purchased from Sigma-Aldrich Corp., St. Louis, MO, USA) from P30. This equates to a daily intake of approximately 80 mg/kg, assuming a 30-g mouse consumes around 5 g food/day. With untreated litters, diet changes were replicated with a control diet (LabDiet 5053 control diet).

### Immunofluorescence

Whole eyes/retinal whole mounts were fixed at room temperature in 4% paraformaldehyde (PFA) for 1.5 hours and 30 minutes, respectively. Following washes, eyes were cryoprotected in 15% sucrose in 1× PBS for 1 hour, 20% sucrose for 1 hour, and 30% sucrose overnight, all at 4°C. Eyes were submerged and frozen in cryochrome (Thermo Fisher Scientific) and sectioned on a cryostat (Leica, Wetzlar, Germany). Sections (7 or 20 μm) were collected on Superfrost glass slides (Thermo Fisher Scientific) and stored at −80°C. Sections were blocked and permeabilized with 0.1% Triton X-100 and 5% donkey serum in 1× PBS for 30 minutes and incubated with primary antibody diluted in 5% donkey serum overnight at 4°C. Retinal whole mounts were blocked and permeabilized with 4% Triton X-100 and 5% donkey serum in 1× PBS for 1.5 hours and incubated with primary antibody overnight at 4°C. The Table lists the details of all primary

antibodies used. Following washes, sections/retinal whole mounts were incubated with secondary antibody (Alexa Fluor donkey anti-mouse/rabbit/goat with either a 488 or a 594 fluorescent probe; Molecular Probes, Eugene, OR, USA) and Hoechst 33342 nuclear stain (1:10,000; Thermo Fisher Scientific) for 1 and 2 hours, respectively, at room temperature. Eliminating the primary antibody in solution served as a negative control. Sections/retinal whole mounts were mounted using Mowiol (Sigma-Aldrich Corp.) with Dabco antifade agent (Sigma-Aldrich Corp.).

## Western Blotting

Whole retinas were homogenized in RIPA buffer (Thermo Fisher Scientific) containing protease and phosphatase inhibitors (Thermo Fisher Scientific). Tissue lysates were centrifuged at 4°C at 15,294*g* for 30 minutes. Supernatant was stored at −80°C. Protein concentration was measured using a Bradford assay (Bio-Rad, Hercules, CA, USA). Next, 4% to 15% gradient gels (Bio-Rad) were used for SDS-PAGE and proteins were then transferred to a nitrocellulose membrane. Protein (20–30 µg) was loaded per sample. Total protein levels are an accurate way of verifying equal loading[31] and so were analyzed using REVERT Total Protein Stain (LiCor, Lincoln, NE, USA) per manufacturer's instructions and imaged on a LiCor scanner in the 700 channel. Membranes were blocked using Odyssey blocking buffer (LiCor) for 30 minutes and probed with primary antibody overnight at 4°C. The Table lists details of the primary antibodies used. Densitometry analysis for proteins of interest was normalized to total protein. Membranes were washed using 1× tris-buffered saline with 1% tween-20 (TBS-T) and probed with IRDye 800CW and 680RD secondary antibodies (LiCor). Membranes were imaged on a LiCor scanner. Densitometry analysis was performed using Image Studio Lite (LiCor).

## Microscopy and Quantification

Retinal sections and cell preparations were viewed using a Leica DM LB2 microscope with Nikon Digital Sight DS-U2 camera (Kanagawa, Japan), using ×10 and ×40 objectives. Images were taken using the software NIS-Elements version 3.0 (Nikon). Confocal micrographs were taken using an Olympus Fluoview FV1000 laser scanning confocal microscope (Shinjuku, Tokyo, Japan), using ×20 and ×40 objectives. Images were taken using the software Olympus Fluoview Ver 4.1a and are represented as maximum-intensity projections from acquisition of z-stacks, inclusive of all retinal layers. All images shown were taken in the central retina. Fluorescence intensity measurements were taken using ImageJ software (National Institutes of Health, Bethesda, MD, USA). Samples were processed at the same time using the same buffers and antibody solutions. Identical microscope settings were used when imaging each preparation across treatment groups, and images were taken in the same session. Numbers of cone arrestin-positive photoreceptors from whole-mount retinas were counted from acquired ×40 images. Numbers of microglia/macrophages from whole-mount retinas included Iba1+ cells with a distinct cell body.

## Phosphoreceptor Tyrosine Kinase Assay

A mouse phospho-RTK array kit was purchased from R&D systems (ARY014; Minneapolis, MN, USA). This kit contains membranes with embedded antibodies against 39 phosphorylated receptor tyrosine kinases (Supplementary Fig. S1). Retinal lysates from P50 rd10 mice on either regular or norgestrel-supplemented diets were prepared using the lysis buffer supplied with the kit along with protease and phosphatase inhibitors (Thermo Fisher Scientific). Protein concentration was measured using a Bradford assay (Bio-Rad). Lysates from three mice per group were pooled to a total of 140 µg. Hence, 140 µg protein was used per membrane and two membranes were used in total (untreated and norgestrel). The array procedure was carried out per manufacturer instructions. Membranes were exposed to X-ray film for 10 minutes.

## Electroretinograph Recordings

Scotopic electroretinograms (ERG) were performed at P50, P60, and P80 in overnight dark-adapted (12 hours) animals. Animals were prepared for bilateral ERG recording under a dim red light. Mice were anesthetized by an intraperitoneal injection of ketamine (100 mg/kg) and xylazine (4 mg/kg), and kept on a thermal blanket at 38°C. Pupils were dilated by topical application of 1% tropicamide (Alcon Cusí, Barcelona, Spain), and 0.2% polyacrylic acid carbomer viscotears (Novartis, Barcelona, Spain) was instilled on the corneas to prevent dehydration and allow electrical contact with the recording electrodes consisting of DTL fiber with an X-Static silver-coated nylon conductive strand (Sauquoit Industries, Scranton, PA, USA). A platinum 25-gauge needle was inserted under the scalp between the eyes as a reference electrode and a gold electrode was placed in the mouth as ground. All the experiments were performed in total darkness in a Faraday cage to avoid external electrical interference. Scotopic ERG responses, in both eyes, were induced by flash light stimuli produced with a Ganzfeld illuminator. Eleven increasing luminances, ranging from −5 to 1 log cd s/m$^2$, of 10-ms duration were presented to the animals at intervals of 10 seconds for dim flashes (−5 to −0.6 log cd s/m$^2$) and 20 seconds for the highest flashes (0–1 log cd s/m$^2$). ERG responses were amplified and band-filtered (1–1000 Hz, without notch filtering) using a DAM50 data acquisition board (World Precision Instruments, Aston, UK). Stimuli presentation and data acquisition at 4 kHz were performed using a PowerLab system (ADInstruments, Oxford, UK). The amplitude of the a-wave was measured from the baseline to the most negative trough, while the amplitude of the b-wave was measured from the trough of the a-wave to the peak of the b-wave.

## Optomotor Testing of Visual Acuity

Visual acuity (VA) evaluation by optomotor testing, related to cone photoreceptor function,[32,33] was assessed at P50, P60, and P80. The assessment of VA was performed using an Argos optomotor system (Instead Technologies, Elche, Spain). The Argos system consists of a chamber created from four computer monitors facing each other forming a square. A charge-coupled device camera with an infrared light lamp in the upper part of the system records the animals placed on a platform in the center of the cube. Mice were allowed to move freely on the platform. The stimuli consisting of black and white bars rotating around the animal were projected in the monitors and were displayed with a frequency of 0.088 cycles/degree for 5 seconds and 100% contrast. The experimenter decided whether the mice performed the tracking motions consisting of a reflexive neck and head movement in the direction of the rotating vertical gratings. The maximum VA corresponded to the spatial frequency threshold obtained by increasing systematically the spatial frequency until the mouse no longer responded.

## Retinal Explant Culture

Retinal explants were prepared from P14 wild-type and P30 rd10 mice. Eyes were enucleated and transferred to a sterile

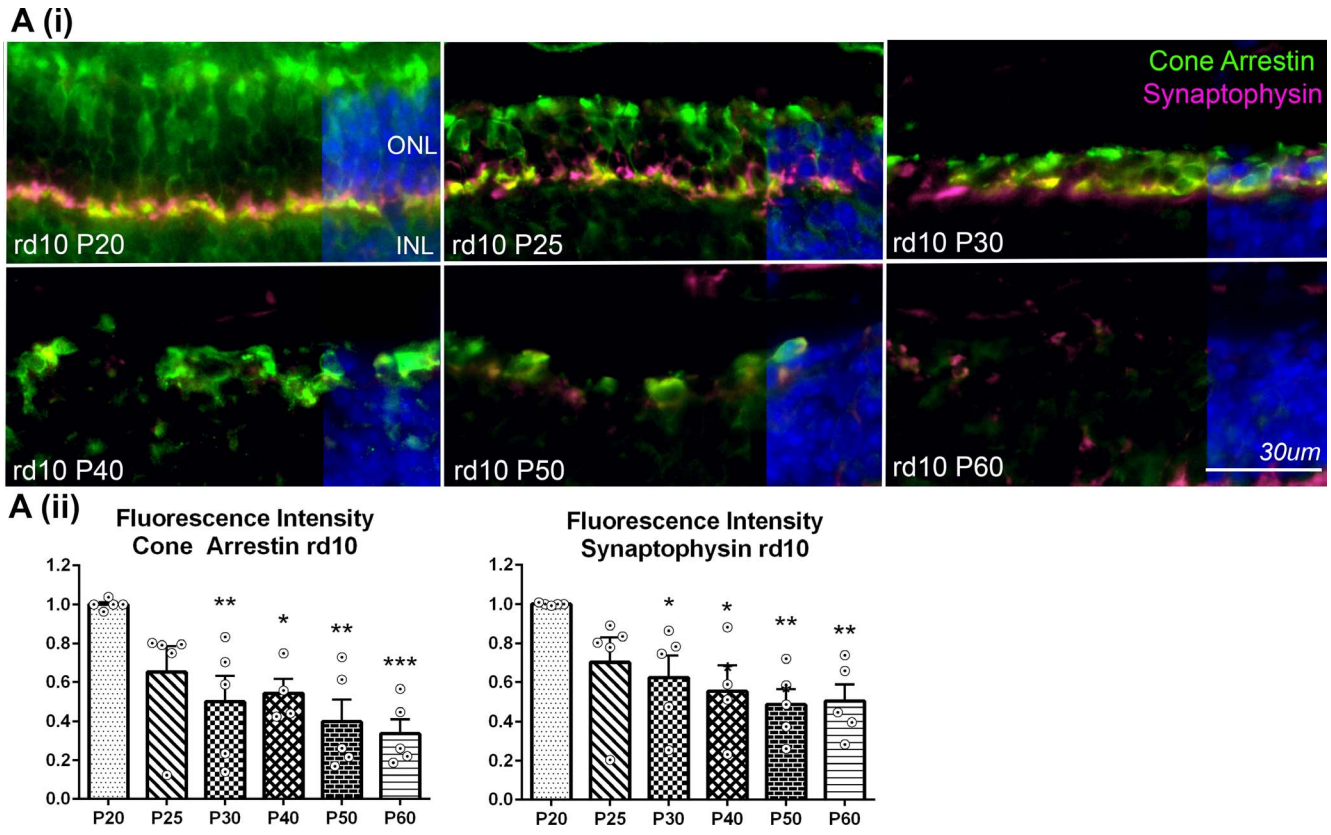


FIGURE 1. The course of cone cell degeneration in the rd10 retina. (**A**) (i) Cone cell morphology (cone arrestin; *green*) and synaptic connectivity in the outer plexiform layer (synaptophysin; *magenta*) decreased in retinal sections from rd10 mice between P20 and P60. Nuclear staining (Hoechst; *blue*) is shown for a small portion of each image to highlight individual cell layers. (**A**) (ii) Quantification of immunofluorescence intensity reveals significant reductions in both cone arrestin and synaptophysin between P25 and P60 compared to P20, in the rd10 retina (1-way ANOVA with Dunnett's multiple comparisons). Data are presented as mean ± SEM; $^{*}P \leq 0.05$, $^{**}P \leq 0.01$, $^{***}P \leq 0.001$; see Supplementary Table S2. INL, inner nuclear layer.

laminar flow hood. Whole retinas were carefully dissected and placed photoreceptor-side down on a cell culture insert in advanced Dulbecco's modified Eagle's medium (DMEM)-F12 (Sigma-Aldrich Corp.) supplemented with 1% penicillin/streptomycin. Retinal explants were cultured for 48 hours in six-well plates with 1.5 mL media per well/explant. Explants were exposed to various concentrations of trametinib (10 mM stock in dimethyl sulfoxide [DMSO]) (ApexBio, Houston, TX, USA) ranging from 10 to 200 nM. All explants were exposed to the same volume of DMSO. The vehicle control was exposed to DMSO alone.

### Experimental Design and Statistical Analysis

The number of animals (*N*) and/or eyes (*n*) used for each experimental analysis is detailed in Supplementary Table S2, along with the type of test used and statistical results. Values in all graphs represent the mean ± standard error of the mean (SEM). Data were statistically analyzed using either unpaired 2-tailed Student's *t*-test or 1-way ANOVA with Dunnett's/Tukey's multiple comparisons (GraphPad, Prism 6; San Diego, CA, USA) with values of $P \leq 0.05$ being considered statistically significant. For ERG and optomotor tests, a 2-way ANOVA (Statistical Package for Social Sciences, Chicago, IL, USA) was used to analyze the functional differences between the groups at different ages (P50, P60, and P80). Post hoc pairwise comparisons using Bonferroni's test were carried out when $P \leq 0.05$. Normal distributions and homogeneity of variance were seen for the categories of the previously defined variables.

## RESULTS

### The Course of Cone Cell Degeneration in the rd10 Retina

In the rd10 retina, rod cell death begins ~P15, and by P25 almost all of the rod photoreceptors have been lost.[26] Changes in cone cell morphology, as visualized by cone arrestin, take place between P20 and P60 (Fig. 1A(i), cone arrestin). Cone cell degeneration progresses by outer segment collapse and cell death. By P60, cone arrestin is sparse in the rd10 retina and a defined outer nuclear layer (ONL) no longer exists (Fig. 1A(i)). Concomitant with the degeneration of cone cells, synaptic connectivity, as assessed by levels of synaptophysin, is lost in the outer plexiform layer (Fig. 1A(i), synaptophysin). Quantification of fluorescence intensity revealed significant reductions in both cone arrestin and synaptophysin between P20 and P60 in the rd10 retina (Fig. 1A(ii)).

### Norgestrel Administration in the Mid-Late Stages of RP Preserves Cone Cells

We administered a norgestrel-supplemented diet to rd10 mice at P30 (Fig. 2A), when rod cells have almost been completely lost[26] and cone cell degeneration has begun (Fig. 1). Assessment of cone cell morphology in retinal sections 20 days later at P50 revealed substantial preservation of cone cells (cone arrestin) as well as synaptic connectivity in the outer plexiform layer (synaptophysin) in norgestrel-fed rd10 mice compared to untreated (Fig. 2B(i)). Measurement of fluores-

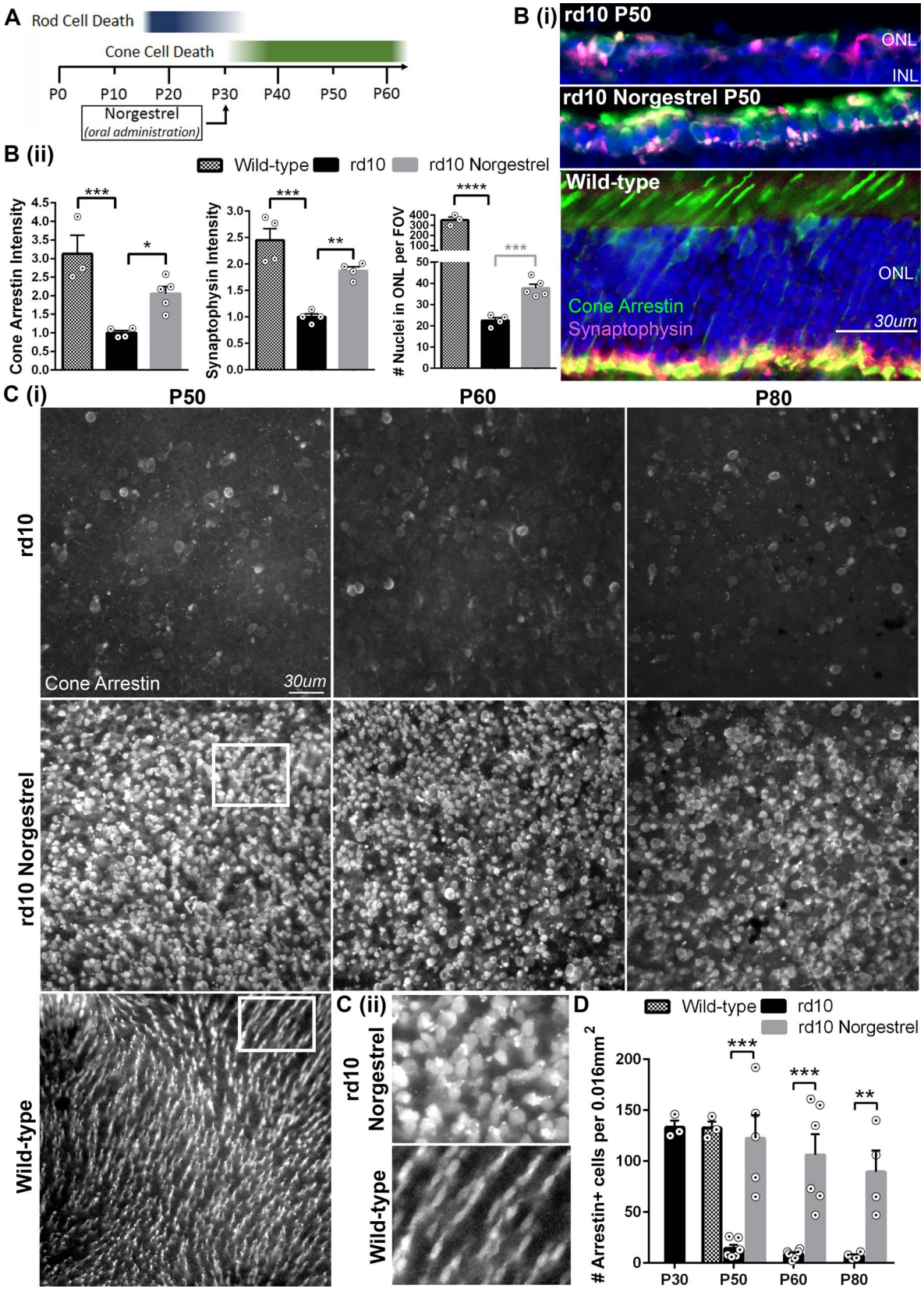


FIGURE 2. Norgestrel administration from P30 preserves cone cells and synaptic connectivity. (**A**) Diet supplementation with norgestrel commenced from P30 in the rd10 mouse, when the majority of rod cells have been lost and cone cell degeneration is beginning. (**B**) (i) Visualization of cone arrestin and synaptophysin at P50 in the rd10 retina revealed a norgestrel-mediated preservation of both cone cells and synaptic connectivity in the outer plexiform layer. Wild-type retina is shown for comparison. (**B**) (ii) Measurement of immunofluorescence intensity confirmed significant increases in cone arrestin and synaptophysin in the norgestrel-treated mice at P50 compared to untreated rd10. Quantification

of the number of nuclei in the ONL confirmed significantly less cells in the rd10 retina compared to wild type (1-way ANOVA with Tukey's multiple comparisons). There were significantly more cells in the ONL of rd10 retinas treated with norgestrel compared to untreated (unpaired Student's *t*-test). This difference was not significant with an ANOVA due to the presence of rods in the wild-type retina, accounting for 95% of photoreceptors. (**C**) (i) Whole-mount retinas from P50, P60, and P80 untreated rd10 mice reveal sparse cone arrestin-positive cells (*white*) whereas rd10 mice on a norgestrel-supplemented diet reveal dense populations at all ages. Whole-mount retina from wild-type P50 is shown for comparison. (**C**) (ii) Higher-magnification images (*white boxes* in **C**[i]) depict differences in cone cell morphology between norgestrel-treated rd10 mice and wild type. (**D**) Quantification of the number of arrestin-positive cells per 0.016 $mm^2$ confirms significantly more cone cells present in the norgestrel-treated rd10 mice compared to age-matched untreated rd10. There was no significant difference between the wild-type and norgestrel-treated rd10 mice at P50 or between the P30 untreated rd10 and P50 norgestrel-treated rd10 (unpaired Student's *t*-test). Data are presented as mean ± SEM; $^{*}P \leq 0.05$, $^{**}P \leq 0.01$, $^{***}P \leq 0.001$, $^{****}P \leq 0.0001$; see Supplementary Table S2.

cence intensity at P50 revealed significant reductions in both cone arrestin and synaptophysin in untreated rd10 retinas compared to wild type, and significant preservation of cones and synapses in the rd10 retina following norgestrel administration (Fig. 2B(ii)). As expected due to the widespread loss of rod photoreceptors, quantification of the number of nuclei in the ONL demonstrated significantly less cells in the P50 rd10 retina compared to wild type. Norgestrel diet supplementation resulted in the presence of significantly more cells in the rd10 ONL compared to untreated (Fig. 2B(ii)).

To gain a greater understanding of the level of neuroprotection offered by norgestrel, we used whole-mount samples to visualize the entire retinal landscape of cone cell morphology. We harvested retinas from P50, P60, and P80 rd10 mice for this analysis and used an antibody against cone arrestin. In the untreated retinas at all ages, cone arrestin-positive cells were sparse (Fig. 2C(i), rd10). In stark contrast, norgestrel-fed mice had far higher densities of cone arrestin-positive cells at all ages (Fig. 2C(i), rd10 norgestrel). Quantification confirmed significantly more cone arrestin-positive cells in the retinas of norgestrel-fed mice at P50, P60, and P80 compared to age-matched untreated (Fig. 2D). Incredibly, up to 28-fold more cone arrestin-positive cells were present following norgestrel treatment (Fig. 2D). Interestingly, this level of cell density in the norgestrel-fed mice at P50 was similar to that in untreated mice at P30 (Fig. 2D), suggesting that little or no degeneration of cone cells occurred once norgestrel administration commenced. In fact, number of cone cells in the norgestrel-fed rd10 mice at P50 was comparable to that of the wild type at P50 (Fig. 2D). As norgestrel treatment resulted in 70% greater numbers of nuclei in the ONL (Fig. 2B(ii)) compared to 770% greater numbers of cone arrestin-positive cells (Fig. 2D) at P50, this indicates that norgestrel's predominant neuroprotective effect is through the preservation of cone cell morphology rather than overall numbers of cone cells. Therefore, norgestrel administration in the mid-late stages of RP immediately halted cone cell degeneration and preserved cone cell morphology for at least a further 50 days, despite the previous widespread loss of rod photoreceptors.

## Norgestrel Preserves Retinal Function

Despite similar densities, a noticeable difference in the morphology of cone cells was observed between wild-type and norgestrel-fed mice at P50 (Figs. 2C(i), white boxes; 2C(ii)). Wild-type cone cells appeared hair-like whereas those in the norgestrel-fed rd10 mice were round (Figs. 2C(i), 2C(ii)). This difference in morphology is not surprising considering the widespread absence of rod photoreceptors and thus structural deficits in the norgestrel-treated retinas from P30.[14] Thus, we sought to determine if the preserved cone cells functioned normally in the norgestrel-fed rd10 mice. Retinal function was assessed in vivo in untreated and norgestrel-fed rd10 mice using ERG recordings and optomotor testing at P50, P60, and P80. ERGs revealed significant preservation of retinal function at P50, P60, and P80 in both a-wave (photoreceptor response) and b-wave amplitudes (response of the inner retina). Wild-type responses at P50 are shown for comparison (Fig. 3A(i)). Example ERG traces depict stronger responses with norgestrel at all ages compared to untreated rd10 mice (Fig. 3A(ii)). Cone cells are responsible for high-level VA, which can be robustly measured using the optomotor test.[32,33] Investigation of retinal function in awake mice using optomotor testing confirmed a significantly higher level of VA in norgestrel-fed mice at P50, P60, and P80 (Fig. 3B). In fact, VA in the norgestrel-treated rd10 mice at P50 was 40% that of the wild-type level. Thus, norgestrel-mediated protection of cone cells importantly transpired to a significant preservation of retinal function.

## Rod Photoreceptors Are Sparse in the Norgestrel-Treated Mice

We wished to delineate the mechanism(s) driving norgestrel-mediated protection of cone cells in the rd10 retina. As discussed in the introduction, cone cells rely heavily on rod cells for trophic support and so we felt it necessary to consider the possible role of norgestrel-mediated protection of remaining rod cells in promoting cone cell protection. As shown in Figure 4, sparse staining of rhodopsin was evident in whole-mount retinas from untreated P50 and P80 rd10 mice in contrast to the strong, dense immunoreactivity observed in the wild-type retina at P50. Rhodopsin immunoreactivity was slightly higher in the norgestrel-treated retinas at P50 and P80 compared to untreated, suggesting marginal protection of the few remaining rod cells (Fig. 4)—albeit, it was clear that rod cell death was widespread in both untreated and norgestrel-treated retinas and that there was a progression of rod cell loss between P50 and P80 with norgestrel. Taking this together with the significant preservation of cone cell morphology and function out to P80, we propose that norgestrel-driven protection of cone cells is unlikely to be solely due to preservation of rod-derived trophic support.

## Norgestrel Does Not Alter Microglial/Macroglial Inflammatory Processes

We have previously demonstrated that norgestrel promotes photoreceptor survival in the early stages of disease by dampening harmful microglial/macroglial processes.[26,28,34] Inflammation might be playing a role in cone cell death[9–11,30,35] and so we studied microglia/macrophage dynamics. Visualization of Iba1+ cells in retinal sections at P50 revealed similar microglia/macrophage numbers, localization, morphology, and phagocytic state (CD68) between untreated and norgestrel-treated mice (Fig. 5A). Analysis of microglia/macrophage number and phagocytic state in z-stacks of whole-mount retinas, inclusive of all layers, supported this result (Fig. 5B(i)) and confirmed similar numbers of microglia/macrophages (Iba1+ cells) and percentages of CD68+ microglia/macrophages between groups (Fig. 5B(ii)). Close to 100% of Iba1+ cells were positive for CD68 in both groups, indicating extensive phagocytic states.

Investigative Ophthalmology & Visual Science

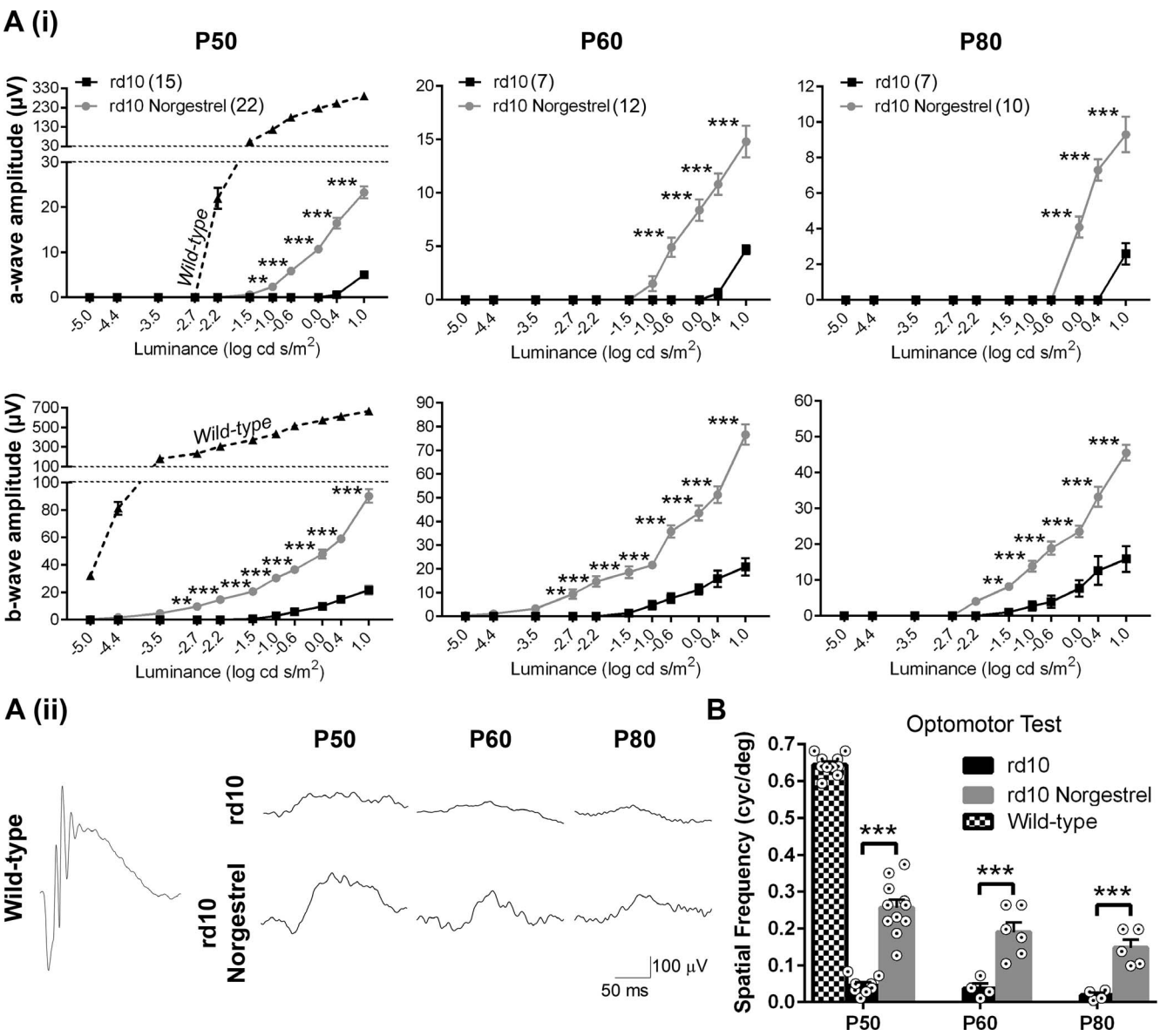


FIGURE 3. Norgestrel preserves retinal function. (**A**) (i) Light intensity response curves of P50, P60, and P80 rd10 mice untreated (*black boxes*) or on norgestrel-supplemented diets (*gray circles*). Wild-type responses at P50 are shown for comparison (*black triangles*). Statistically significant increases were observed in rd10 retinas with norgestrel, in both a-wave and b-wave amplitudes at all ages, compared to untreated (2-way ANOVA with Bonferroni's pairwise comparisons). (**A**) (ii) Representative ERG waveforms performed on untreated rd10 and norgestrel-fed rd10 mice at P50, P60, and P80 indicating increased neurotransmission in the rd10 retina with norgestrel. An ERG trace from a wild-type adult is shown for comparison. (**B**) Visual acuity measured by the optomotor test revealed significant increases with norgestrel at P50, P60, and P80 compared to untreated rd10 (unpaired Student's *t*-test). Wild-type visual acuity is shown at P50 for comparison. Data are presented as mean ± SEM; $^{**}P \leq 0.01$, $^{***}P \leq 0.001$; see Supplementary Table S2 for details.

Our previous work on macroglial activity in the diseased retina has shown that norgestrel significantly reduces Müller cell gliosis,[34] a process believed to impede tissue repair and remodeling following injury.[36,37] We therefore investigated the possibility that norgestrel was using this mechanism to protect cone cells. Assessment of Müller cell gliosis by glial fibrillary acidic protein (GFAP) immunoreactivity in retinal sections, a well-characterized marker of gliosis,[36,37] alongside glutamine synthetase (a Müller cell–specific protein) revealed similar levels between untreated and norgestrel-treated mice at P50 (Fig. 6A(i)). GFAP is also expressed by astrocytes in the retina, which reside in the retinal ganglion cell layer. Z-stacks of GFAP immunoreactivity in whole-mount retinas presented a typical stellate astrocytic morphology, with similar levels of GFAP throughout the retina (Fig. 6A(ii)). Western blot analysis for GFAP and glutamine synthetase levels confirmed that gliosis is unaffected by norgestrel treatment (Fig. 6B). Taken together with the data in Figure 5, these results suggest that norgestrel is not targeting either microglia/macrophage or macroglia inflammatory processes to promote preservation of cone cells.

## Norgestrel Does Not Affect Oxidative Stress

As oxidative stress is a major contributing factor to cone cell loss in RP,[5–7,38,39] and norgestrel is known to alleviate oxidative stress in a light-damage model of retinal degeneration via upregulation of antioxidant enzymes,[25] we investigated anti-oxidative mechanisms as a possible neuroprotective strategy

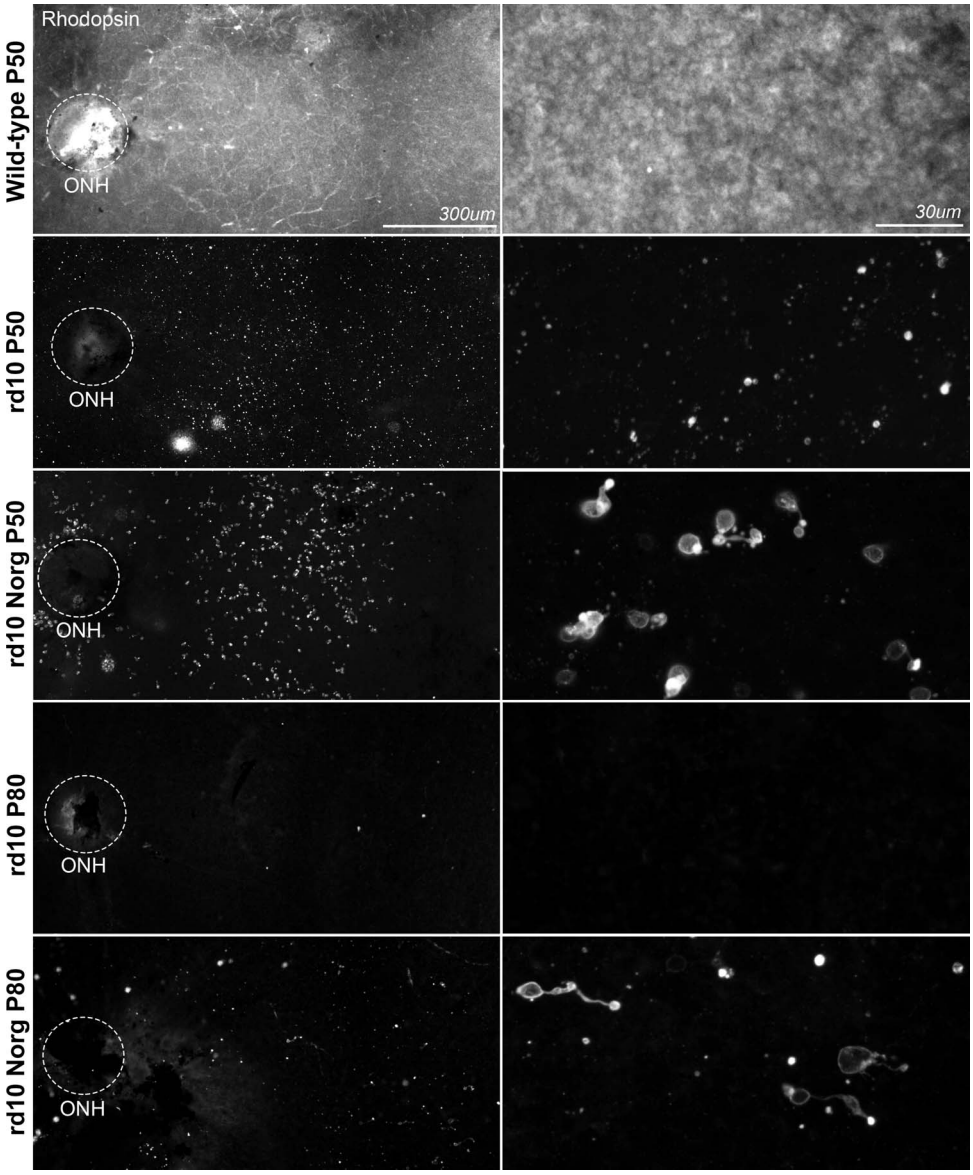


FIGURE 4. Rod cells are sparse in the norgestrel-treated rd10 retinas. Rhodopsin staining in whole-mount untreated rd10 retina is sparse at P50 and absent at P80, as demonstrated by both low- and high-magnification images. Wild-type P50 retinas are shown for comparison and show intense and dense rhodopsin staining. Rhodopsin staining is also sparse in the norgestrel-treated mice at P50 and P80 although some cell bodies can be observed. The optic nerve head (ONH) is shown by a *dotted circle*. *Scale bars* represent 300 and 30 μm.

against cone cell degeneration. First, we assessed levels of acrolein, a reactive aldehyde and marker of oxidative stress in the diseased retina. Acrolein immunoreactivity was strongest in the outer retina in both untreated and norgestrel-treated mice at P50 and similar levels were observed between groups (Fig. 7A), suggesting that norgestrel does not reduce oxidative stress to combat cone cell degeneration. In line with this, we did not see any increase in the antioxidative enzymes SOD1, SOD2, catalase, glutathione reductase, and glutathione peroxidase with norgestrel (Fig. 7B). In fact, we found significant decreases in levels of SOD1 and SOD2 with norgestrel (Fig. 7B(ii)).

Oxidative stress can promote mitochondrial damage and subsequent apoptosis.[37,40,41] Bcl-2 is an antiapoptotic protein located at the mitochondrial outer membrane and works by inhibiting the proapoptotic protein Bax. Mitochondrial-induced apoptosis occurs via activation of caspases 3 and 9.[40,41] Bax-mediated cell death has been demonstrated in models of RP,[42] and progestins are known to increase mRNA levels of Bcl-2 via interaction of the progesterone receptor to the Bcl-2 promoter.[43] We therefore investigated the possibility that norgestrel was preventing the damaging effects of oxidative stress at the level of Bcl-2. This was shown not to be the case, as Western blot analysis revealed similar levels of Bcl-2 and its target Bax between groups at P50, along with caspase 3 and caspase 9 (Fig. 7C).

## Norgestrel Stimulates ERK1/2 Signaling in Müller Glial Cells

Our group has published several studies highlighting a norgestrel-mediated upregulation of growth factors that promotes photoreceptor survival.[27,44–46] Growth factors mediate their effects via binding to receptor tyrosine kinases.[47] We therefore turned our attention to growth factor signaling as a mechanism for norgestrel-driven protection of cone cells in

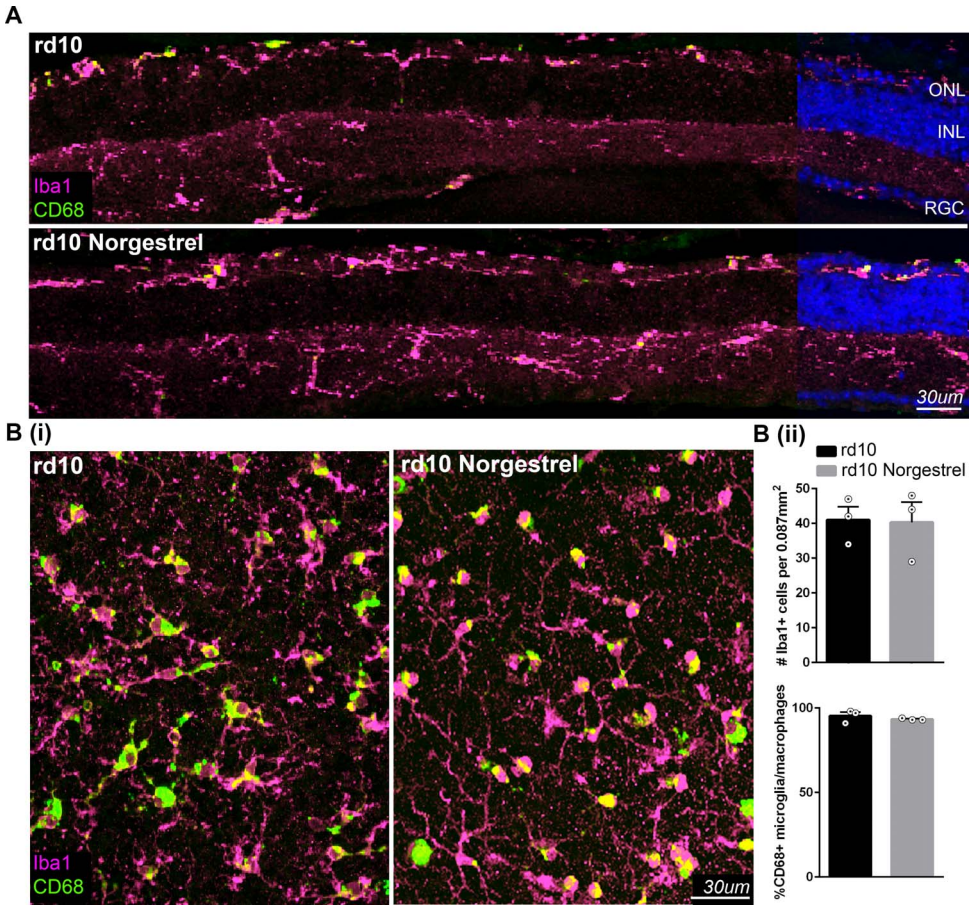


**Figure 5.** Norgestrel does not affect microglia/macrophage numbers, morphology, or phagocytic states. (**A**) Visualization of microglia/macrophages (Iba1; *magenta*) alongside a marker of phagocytosis (CD68; *green*) reveals similar numbers, morphology, localization, and phagocytic states in retinal sections from untreated and norgestrel-treated mice at P50. Nuclear staining (Hoechst; *blue*) is shown for a small portion of each image to highlight individual cell layers. (**B**) (i) Whole-mount retinas from P50 mice, inclusive of all retinal layers, reveal similar numbers, morphology, and phagocytic states of Iba1+ cells between untreated and norgestrel. (**B**) (ii) Quantification of Iba1+ cells and CD68+ cells confirms no significant difference between groups (unpaired Student's *t*-test). Data are presented as mean ± SEM; see Supplementary Table S2 for details. RGC, retinal ganglion cells.

the rd10 retina. To study this thoroughly, we used a phosphoreceptor tyrosine kinase array in which antibodies for 39 receptor tyrosine kinases are represented on a single membrane (see Methods for full details and Supplementary Fig. S1). This revealed an interesting result in that the receptor with the highest level of activation in both untreated and norgestrel-treated P50 retinas was ErbB2 (analogous with human ERBB2/HER2) (Supplementary Fig. S1). More interesting still, norgestrel-treated retinas had a ~100% increase in ErbB2 activity compared to untreated (Fig. 8A). ErbB2 is a member of the epidermal growth factor (EGF) family of receptors. Activation of ErbB2 leads to downstream activation of Akt and extracellular signal-related kinase 1 and 2 (ERK1/2), pathways involved in cell survival and proliferation. Western blot analysis of pAkt and its downstream target mammalian target of rapamycin (mTOR) did not show any change with norgestrel (Figs. 8B(i), 8B(ii)). However, both pERK1 and pERK2 were significantly increased with norgestrel (Figs. 8B(i), 8B(ii)). An increase in pMEK1/2, an upstream regulator of pERK1/2, was also observed (Figs. 8B(i), 8B(ii)).

Using whole-mount retinas from P50 mice, a norgestrel-dependent increase in pERK1/2 was confirmed by immunofluorescence with clear cluster-like areas of strong immunoreactivity (Fig. 8C(i)). In order to determine the cellular location of pERK1/2, pERK1/2 was first visualized alongside cone arrestin in norgestrel-treated retinas. It was clear that pERK1/2 did not colocalize with cone arrestin and instead depicted a Müller glial cell morphology (Fig. 8C(ii)). To confirm this, pERK1/2 was visualized alongside GFAP, and indeed there was some level of colocalization (Fig. 8C(ii)). Hence, treatment with norgestrel resulted in an upregulation of ErbB2 activity in the rd10 retina, a receptor tyrosine kinase strongly implicated in cell proliferation, differentiation, and survival. An increase in ERK1/2 signaling, a well-studied consequence of ErbB2 activation, was observed in Müller glia.

## ERK1/2 Signaling Is Critical for Norgestrel-Mediated Neuroprotection of Cone Cells

We hypothesized that ERK1/2 signaling was playing a crucial role in norgestrel-mediated neuroprotection of cone photoreceptors in the rd10 retina. To investigate this, we wished to administer norgestrel in combination with an inhibitor of ERK1/2 signaling. Trametinib is a MEK1/2 inhibitor, which consequently prevents phosphorylation and thereby activity of ERK1/2.[48–51] Using retinal explants from wild-type mice, we administered various concentrations of trametinib (10, 50, 100, and 200 nM) over 48 hours and found that all concentrations resulted in significant decreases in levels of pERK1/2 compared to vehicle, whereas total ERK1/2 remained unchanged, as assessed by Western blot (Fig. 9A). The lowest levels of pERK1/2 were observed with 100 nM trametinib (Fig.

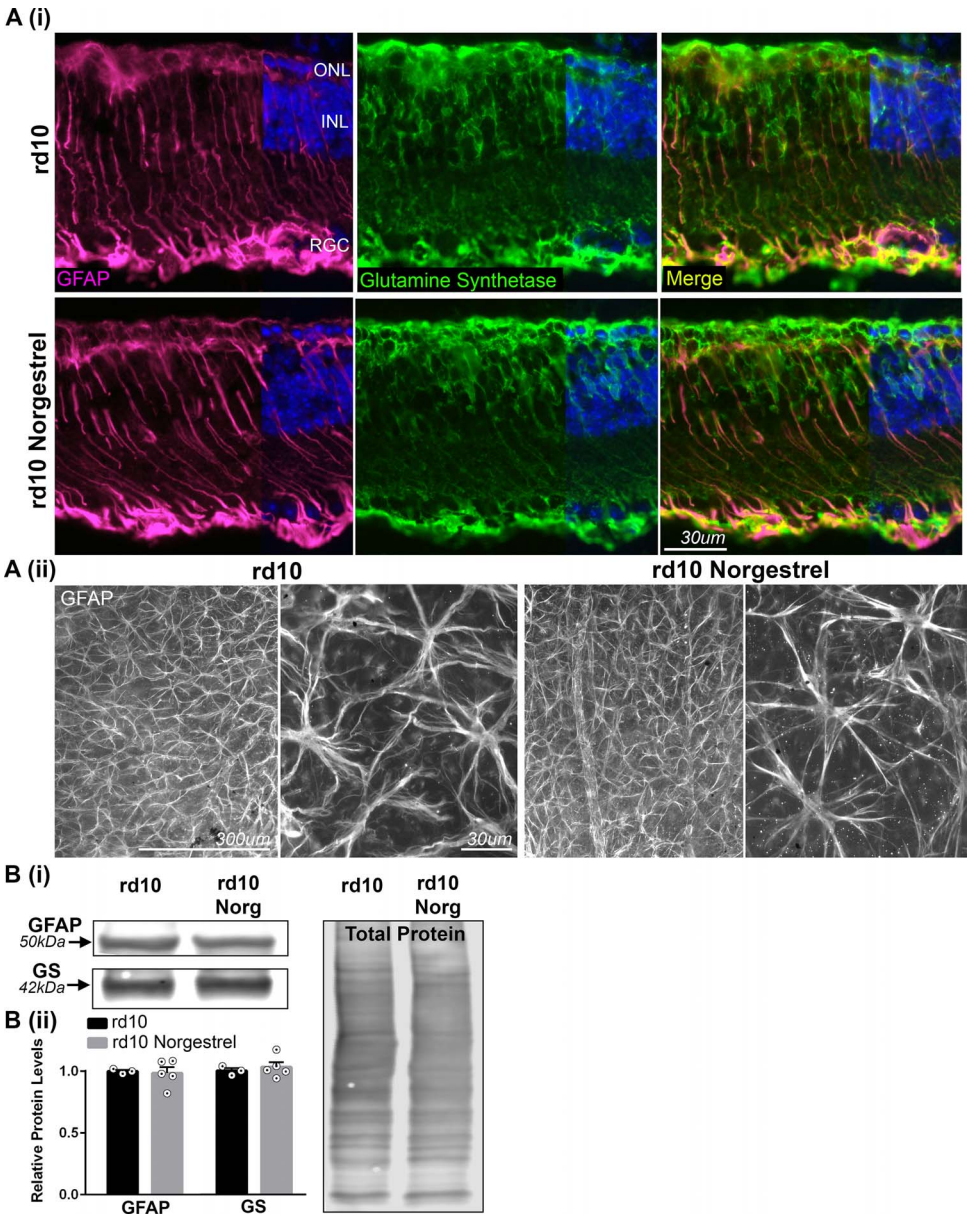


**Figure 6.** Norgestrel does not alter levels of GFAP. (**A**) (i) Assessment of Müller cell morphology (glutamine synthetase [GS]; *green*) and gliosis (GFAP; *magenta*) in retinal sections from P50 untreated and norgestrel-treated mice showed similar results. Nuclear staining (Hoechst; *blue*) is shown for a small portion of each image to highlight individual cell layers. (**A**) (ii) Whole-mount retinal analysis of GFAP at P50, inclusive of all retinal layers, revealed similar levels and morphology of GFAP immunoreactivity. Astrocytes can be observed by their typical stellate appearance. (**B**) (i) Western blot analysis supported immunofluorescent findings and (**B**) (ii) confirmed similar levels of GFAP and glutamine synthetase (GS) between untreated and norgestrel-treated mice at P50 (unpaired Student's *t*-test). REVERT Total Protein Stain demonstrates equal loading of samples. Data are presented as mean ± SEM; see Supplementary Table S2 for details. RGC, retinal ganglion cells.

9A(ii)). To ascertain the role of ERK1/2 signaling in norgestrel-mediated neuroprotection of cone cells in the rd10 retina, retinal explants were prepared from P30 rd10 mice and treated with either vehicle, norgestrel, or norgestrel + trametinib over 48 hours. Norgestrel-treated retinas retained significantly higher numbers of arrestin-positive cells compared to vehicle, as visualized and quantified in whole-mount preparations (Fig. 9B). Treatment of rd10 retinal explants with norgestrel in the presence of trametinib prevented this neuroprotective effect (Fig. 9B). Quantification of arrestin-positive cells confirmed a critical role for ERK1/2 signaling in norgestrel-driven neuroprotection of cone cells (Fig. 9B(ii)).

## Discussion

This study was designed to investigate the long-term neuroprotective potential of norgestrel, a synthetic progestin, when administered in the mid-late stages of RP when the majority of rod cells have already been lost and cone cell degeneration is beginning. Investigations of therapeutic interventions that are effective at this stage of the disease are critical, considering that rod cell death can go unnoticed for some time along with the debilitating effects of cone cell loss on daytime vision. In the rd10 retina at P30, rod cell death is almost complete and cone degeneration has begun[14] (Figs. 1, 2). As rod cells

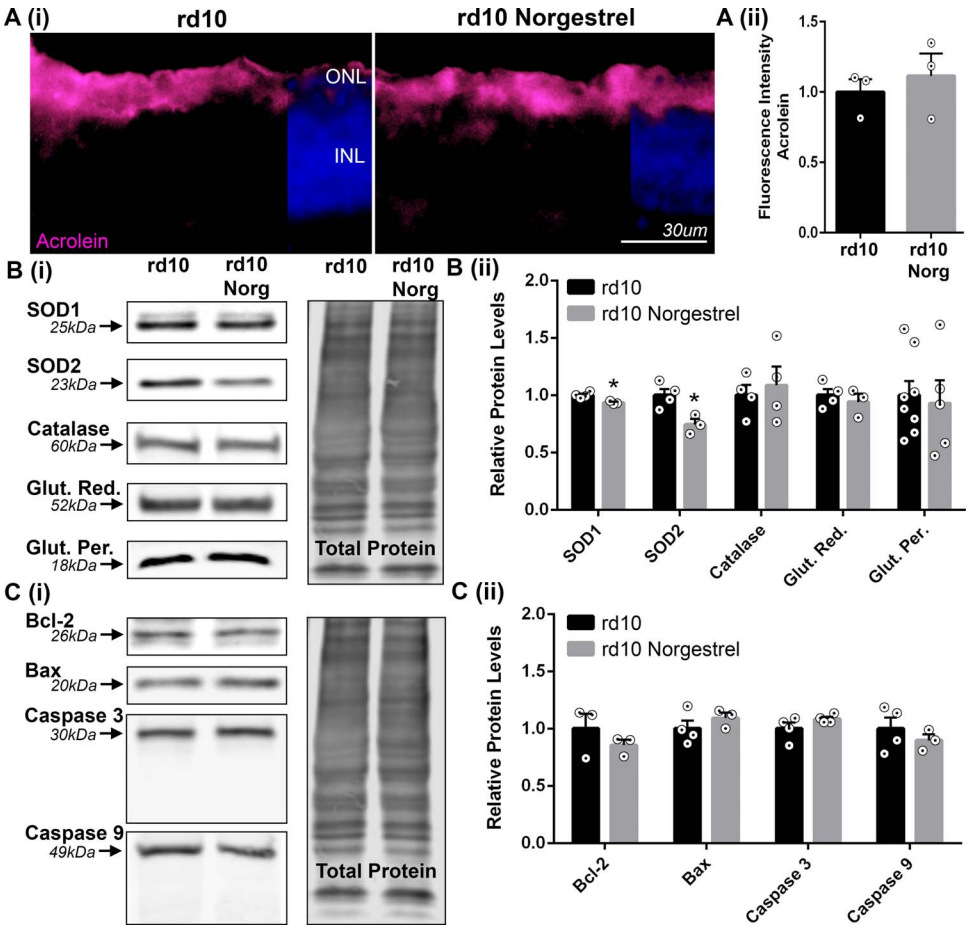


FIGURE 7. Norgestrel does not alter levels of oxidative stress. (**A**) (i) Acrolein was visualized as a marker of oxidative stress and was observed in the outer retina, at similar levels in untreated and norgestrel-treated mice at P50. (**A**) (ii) Measurement of immunofluorescence intensity confirmed similar levels of acrolein between groups (unpaired Student's *t*-test). (**B**) (i) Western blot analysis for antioxidant enzymes demonstrated similar levels of catalase, glutathione reductase, and glutathione peroxidase between untreated and norgestrel-treated retinas at P50. SOD1 and SOD2 levels were lower with norgestrel. REVERT Total Protein Stain demonstrates equal loading of samples. (**B**) (ii) Densitometry analysis confirmed norgestrel-driven decreases in SOD1 and SOD2 and similar levels of catalase, glutathione reductase, and glutathione peroxidase between groups (unpaired Student's *t*-test). (**C**) (i) Western blot analysis for Bcl-2, Bax, caspase 3, and caspase 9 demonstrated similar levels between untreated and norgestrel-treated retinas at P50. REVERT Total Protein Stain demonstrates equal loading of samples. (**C**) (ii) Densitometry analysis confirmed similar levels of Bcl-2, Bax, caspase 3, and caspase 9 between groups (unpaired Student's *t*-test). Data are presented as mean ± SEM; $^*P \leq 0.05$; see Supplementary Table S2 for details.

account for at least 95% of photoreceptors,[3,52] the P30 retina has undergone considerable cell death and widespread structural alterations.

Administration of a norgestrel-supplemented diet to rd10 mice from P30 resulted in profound neuroprotection of existing cone cells in the following 50 days, with the number of cone arrestin-positive cells almost 13-fold higher than in untreated at P80 (Fig. 2D). As norgestrel treatment resulted in 70% greater numbers of nuclei in the ONL (Fig. 2B) compared to 770% greater numbers of cone arrestin-positive cells (Fig. 2D) at P50, we propose that norgestrel predominantly protects cone cell morphology. A similar effect has been previously reported following administration of ciliary neurotrophic factor (CNTF) in a rat model of RP.[53] Critically, this protection of cone cells transpired to a significant preservation of retinal function as measured by ERG recordings and optomotor testing (Fig. 3). Interestingly, although P50 wild-type ERG responses are far higher compared to rd10 treated with norgestrel, measures of VA in awake mice were much closer between the two groups, indicating a high degree of vision overall (Fig. 3). Hence, norgestrel could potentially be used in both the early[26] and mid-late stages (current study) of the disease. Critically, it could provide long-term protection of cone cells and preservation of color/daytime vision.

Previous work has demonstrated the ability of norgestrel to promote photoreceptor survival and preserve retinal function when administered prior to photoreceptor loss in the rd10 mouse.[26] Our work has shown that norgestrel orchestrates a strong neuroprotective defense against the underlying disease by utilizing multiple signaling pathways and targeting several cell types. Norgestrel dampens harmful microglia/macrophage activity, gliosis, and oxidative stress in the early stages of the disease.[25,26,28,34] Surprisingly, although high levels of microglial/macrophage activity, gliosis, and oxidative stress were observed in the rd10 retina during cone cell degeneration, norgestrel administration did not reduce any of these effects (Figs. 5–7). We propose that such processes are more strongly associated with rod cell death and its aftermath, and are not the predominant driving forces of cone cell degeneration in RP, as norgestrel promoted remarkable protection of cones despite prevailing inflammation and oxidative stress. In fact, we observed significant reductions in levels of the antioxidant enzymes SOD1 and SOD2 in the norgestrel-treated mice (Fig. 7). This could be due to a healthier retina requiring less

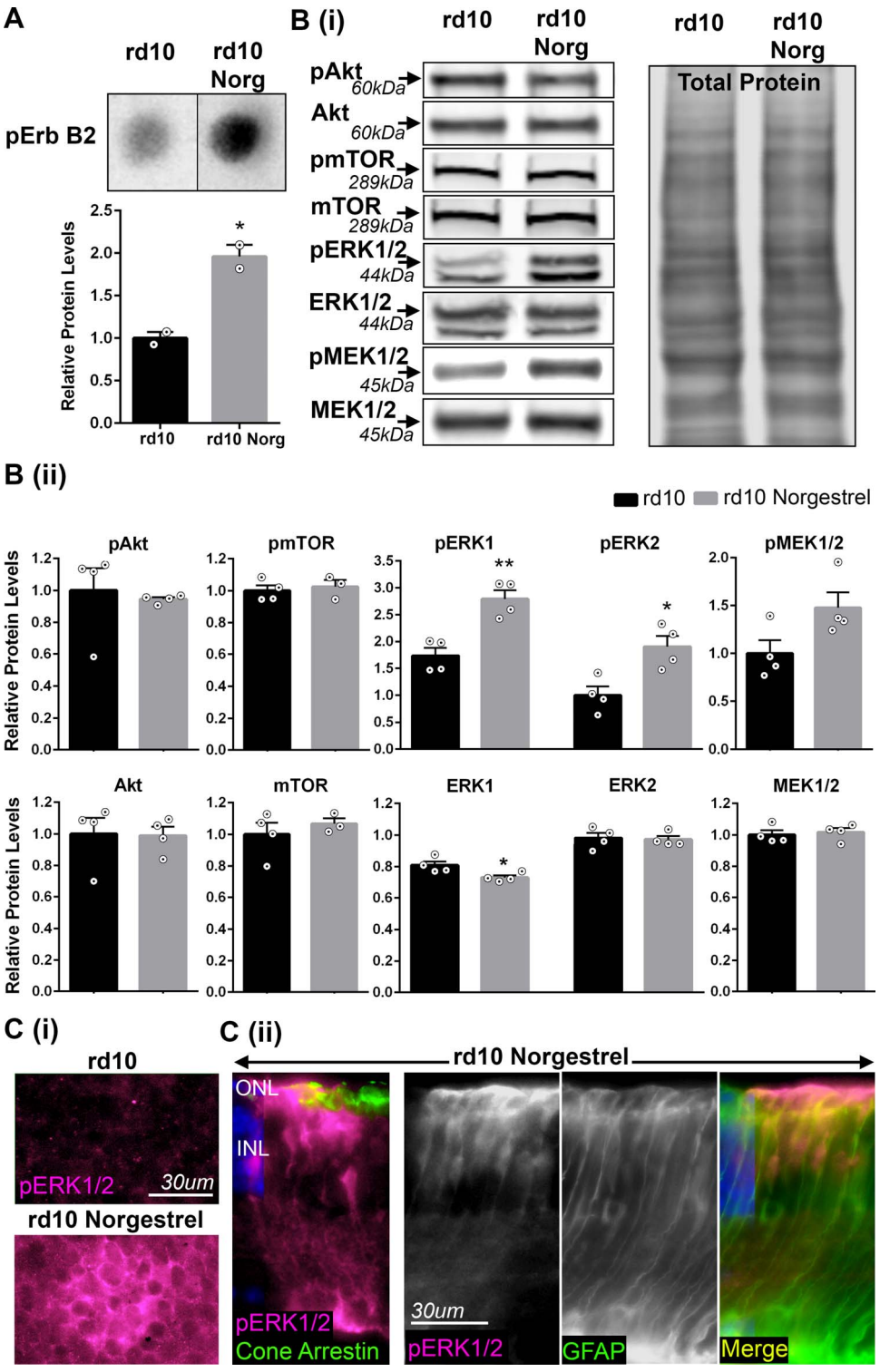


FIGURE 8. Norgestrel administration results in increased activation of ErbB2 and ERK1/2. (**A**) Using a receptor-tyrosine kinase activity array, significantly increased levels of activated ErbB2 were found in retinas from norgestrel-treated rd10 mice compared to untreated at P50. (**B**) (i) Assessment of components of the Akt and ERK1/2 pathways by Western blot at P50 demonstrates unchanged activity of the Akt pathway (pAkt, Akt, pmTOR, and mTOR) whereas clear increases in levels of pERK1/2 and pMEK1/2 are seen. REVERT Total Protein Stain demonstrates equal loading of samples. (**B**) (ii) Densitometry analysis confirms significant increases in pERK1 and pERK2 following norgestrel treatment (unpaired Student's *t*-test). (**C**) (i) An increase in pERK1/2 with norgestrel was observed in whole-mount retinas and appeared in clusters. (**C**) (ii) Investigations on the cellular location of pERK1/2 revealed an absence of pERK1/2 in cone photoreceptors (pERK1/2 and cone arrestin) and a high level of colocalization in Müller glia (pERK1/2 and GFAP). Nuclear staining (Hoechst; *blue*) is shown for a small portion of each image to highlight individual cell layers. Data are presented as mean ± SEM; $^{*}P \leq 0.05$, $^{**}P \leq 0.01$; see Supplementary Table S2 for details.

Investigative Ophthalmology & Visual Science

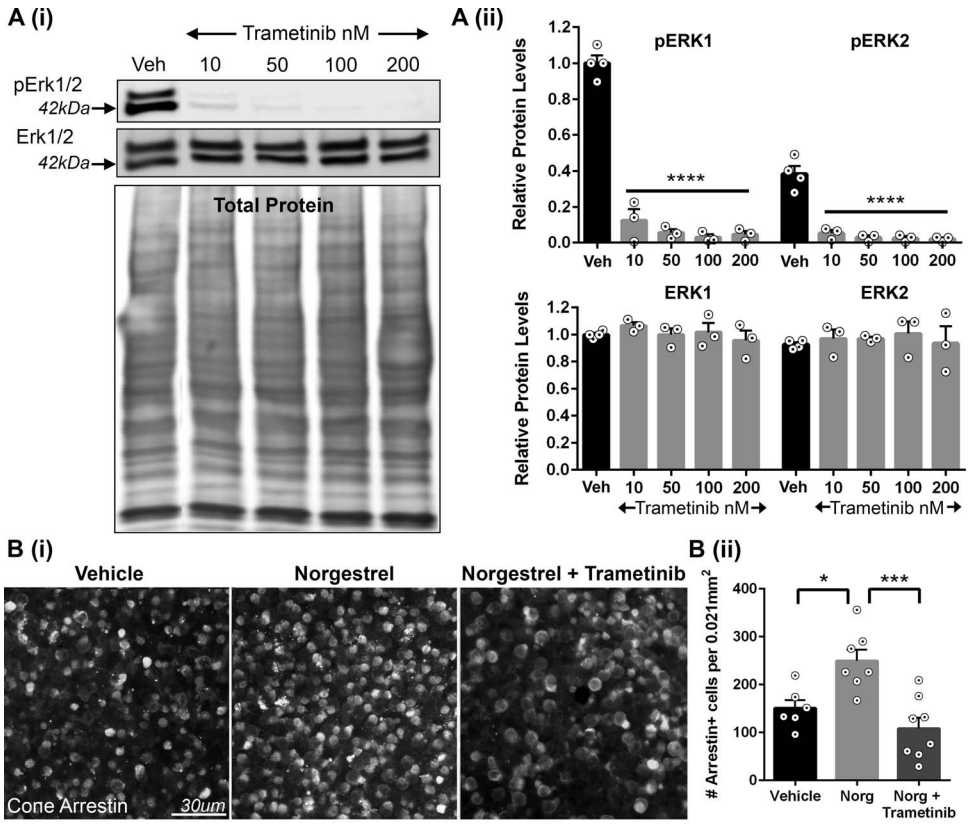


**Figure 9.** ERK1/2 signaling is critical for norgestrel-mediated protection of rd10 cone photoreceptors. (**A**) (i) Exposing wild-type retinal explants to increasing doses of trametinib (a MEK inhibitor) for 48 hours, ranging from 10 to 200 nM, resulted in significant decreases in pERK1/2 whereas levels of total ERK1/2 remained unchanged. REVERT Total Protein Stain demonstrates equal loading of samples. (**A**) (ii) Densitometry analysis confirmed significant trametinib-driven decreases in both pERK1 and pERK2 at all doses (1-way ANOVA with Dunnett's multiple comparisons). (**B**) (i) Whole-mount retinal explants from P30 rd10 mice cultured for 48 hours reveal sparse cone arrestin staining (*white*) in vehicle treated whereas norgestrel treatment protected cone photoreceptors. Administration of norgestrel in combination with trametinib attenuated norgestrel's protective effects. (**B**) (ii) Quantification of the number of arrestin-positive cells per 0.021 $mm^2$ confirms significantly more cone cells present in the norgestrel-treated rd10 mice compared to untreated. There was a significant reduction in the number of arrestin+ cells when norgestrel was administered in combination with trametinib (1-way ANOVA with Tukey's multiple comparisons). Data are presented as mean ± SEM; $^{*}P \leq 0.05$, $^{***}P \leq 0.001$, $^{****}P \leq 0.0001$; see Supplementary Table S2 for details.

antioxidant defenses. Although there is some evidence for mitochondrial damage and subsequent activation of apoptotic pathways in animal models of RP,[42] this was observed in the early stages of the disease, prior to or during rod cell death. Hence, it is possible that these pathways either are not implicated or are not the dominant driving force behind cone cell loss (Fig. 7). In addition, we conclude that norgestrel is not mediating its effects via insulin/mTOR signaling, a pathway implicated in cone cell death and survival in RP.[8] We did not detect any activation of insulin receptors in either the untreated or norgestrel-treated retinas (Supplementary Fig. S1). In line with this, we did not observe any change in the activation of mTOR (Fig. 8B).

Our studies on the possible role of growth factor signaling in norgestrel-mediated neuroprotection presented a new and exciting result. ErbB2 receptor activity was significantly upregulated with norgestrel (Fig. 8). ErbB2 (analogous with human ERBB2/HER2) belongs to the family of EGF receptors and has been widely studied in the field of cancer research.[54] Elevated ErbB2 activity is a hallmark of many cases of breast cancer and has been shown to drive signaling pathways for cell survival, differentiation, and proliferation.[54] Progestins have previously been shown to increase EGF receptor activity and its downstream pathways in breast cancer cells.[55,56] This could be due to the autocrine actions of progesterone receptors as transcription factors for EGF receptors and their ligands.[55,57]

A major signaling pathway driven by activation of ErbB2 is the MAP-kinase or ERK1/2 pathway, which has been demonstrated to drive differentiation and proliferation.[54] It was interesting to see an increase in ERK1/2 activity in Müller glia specifically (Fig. 8C) considering that these cells have the capacity to dedifferentiate into neuronal cells following retinal injury and neuronal loss.[58] In chick and fish retinas, Müller glia undergo dedifferentiation and can successfully replace lost neurons. In the mammalian retina, however, Müller glia initiate the dedifferentiation process but fail to fully function as retinal progenitors.[58] Interestingly, Müller glia in the mammalian retina can be encouraged to proliferate and dedifferentiate with certain molecular cues.[59–61] One of the most potent methods for stimulating Müller glial proliferation in the mammalian retina is treatment with EGF, a ligand for the ErbB family of receptors.[59,60,62] When ERK1/2 activity was inhibited in mouse retinal explants, EGF could no longer stimulate Müller glial proliferation.[60] EGF-ERK1/2 signaling is known to occur as part of Müller glial proliferation and dedifferentiation in fish retina also.[63] Through the inhibition of ERK1/2 ex vivo, we demonstrated that ERK1/2 signaling is critical for norgestrel-mediated preservation of cone cells in the rd10 retina (Fig. 9). We hope to further explore the role of Müller glia and

ERK1/2 signaling in norgestrel-driven preservation of cone cells in the near future.

Taken as a whole, this study presents a promising treatment for RP in the form of norgestrel, a synthetic progestin. Norgestrel can protect existing cone photoreceptors and retinal function for at least 50 days in the rd10 mouse even if administered in the mid-late stages of the disease, when rod cells have almost been completely lost and cone cell degeneration has begun. Thus, norgestrel could potentially be used to prevent cone cell degeneration and maintain color vision for those living with RP.

## *Acknowledgments*

The authors thank the animal facility staff in the Biological Services Unit University College Cork for their support and caring for the animals used in this study.

Supported by grants from Science Foundation Ireland (SFI 13/IA/1783), Fighting Blindness Ireland (FB13COT), Spanish Ministry of Economy and Competitiveness (MINECO-FEDER-BFU2015-67139-R), Generalitat Valenciana (Prometeo 2016/158), and Carlos III Institute (ISCIII RETICS-FEDER RD16/0008/0016).

Disclosure: **S.L. Roche**, None; **O. Kutsyr**, None; **N. Cuenca**, None; **T.G. Cotter**, None

## *References*

1. Daiger SP, Sullivan LS, Bowne SJ, Rossiter BJF. RetNet, the Retinal Information Network. Available at: https://sph.uth.edu/retnet/.
2. Verbakel SK, van Huet RAC, Boon CJF, et al. Non-syndromic retinitis pigmentosa. *Prog Retin Eye Res*. 2018;66:157–186.
3. Curcio CA, Sloan KR, Kalina RE, Hendrickson AE. Human photoreceptor topography. *J Comp Neurol*. 1990;292:497–523.
4. Ait-Ali N, Fridlich R, Millet-Puel G, et al. Rod-derived cone viability factor promotes cone survival by stimulating aerobic glycolysis. *Cell*. 2015;161:817–832.
5. Komeima K, Rogers BS, Campochiaro PA. Antioxidants slow photoreceptor cell death in mouse models of retinitis pigmentosa. *J Cell Physiol*. 2007;213:809–815.
6. Shen J, Yang X, Dong A, et al. Oxidative damage is a potential cause of cone cell death in retinitis pigmentosa. *J Cell Physiol*. 2005;203:457–464.
7. Campochiaro PA, Mir TA. The mechanism of cone cell death in retinitis pigmentosa. *Prog Retin Eye Res*. 2018;62:24–37.
8. Punzo C, Kornacker K, Cepko CL. Stimulation of the insulin/mTOR pathway delays cone death in a mouse model of retinitis pigmentosa. *Nat Neurosci*. 2009;12:44–52.
9. Viringipurampeer IA, Metcalfe AL, Bashar AE, et al. NLRP3 inflammasome activation drives bystander cone photoreceptor cell death in a P23H rhodopsin model of retinal degeneration. *Hum Mol Genet*. 2016;25:1501–1516.
10. Yoshida N, Ikeda Y, Notomi S, et al. Clinical evidence of sustained chronic inflammatory reaction in retinitis pigmentosa. *Ophthalmology*. 2013;120:100–105.
11. Murakami Y, Ikeda Y, Nakatake S, et al. Necrotic enlargement of cone photoreceptor cells and the release of high-mobility group box-1 in retinitis pigmentosa. *Cell Death Discov*. 2015;1:15058.
12. Chang B, Hawes NL, Hurd RE, et al. Retinal degeneration mutants in the mouse. *Vis Res*. 2002;42:517–525.
13. Hartong DT, Berson EL, Dryja TP. Retinitis pigmentosa. *Lancet*. 2006;368:1795–1809.
14. Roche SL, Wyse-Jackson AC, Byrne AM, Ruiz-Lopez AM, Cotter TG. Alterations to retinal architecture prior to photoreceptor loss in a mouse model of retinitis pigmentosa. *Int J Dev Biol*. 2016;60:127–139.
15. Barhoum R, Martinez-Navarrete G, Corrochano S, et al. Functional and structural modifications during retinal degeneration in the rd10 mouse. *Neuroscience*. 2008;155:698–713.
16. Gargini C, Terzibasi E, Mazzoni F, Strettoi E. Retinal organization in the retinal degeneration 10 (rd10) mutant mouse: a morphological and ERG study. *J Comp Neurol*. 2007;500:222–238.
17. Yang Y, Mohand-Said S, Danan A, et al. Functional cone rescue by RdCVF protein in a dominant model of retinitis pigmentosa. *Mol Ther*. 2009;17:787–795.
18. Oveson BC, Iwase T, Hackett SF, et al. Constituents of bile, bilirubin and TUDCA, protect against oxidative stress-induced retinal degeneration. *J Neurochem*. 2011;116:144–153.
19. Fernandez-Sanchez L, Lax P, Pinilla I, Martin-Nieto J, Cuenca N. Tauroursodeoxycholic acid prevents retinal degeneration in transgenic P23H rats. *Invest Ophthalmol Vis Sci*. 2011;52:4998–5008.
20. Fernandez-Sanchez L, Lax P, Esquiva G, et al. Safranal, a saffron constituent, attenuates retinal degeneration in P23H rats. *PLoS One*. 2012;7:e43074.
21. Wang J, Saul A, Roon P, Smith SB. Activation of the molecular chaperone, sigma 1 receptor, preserves cone function in a murine model of inherited retinal degeneration. *Proc Natl Acad Sci U S A*. 2016;113:E3764–E3772.
22. Fernandez-Sanchez L, Bravo-Osuna I, Lax P, et al. Controlled delivery of tauroursodeoxycholic acid from biodegradable microspheres slows retinal degeneration and vision loss in P23H rats. *PLoS One*. 2017;12:e0177998.
23. Noailles A, Fernandez-Sanchez L, Lax P, Cuenca N. Microglia activation in a model of retinal degeneration and TUDCA neuroprotective effects. *J Neuroinflammation*. 2014;11:186.
24. Doonan F, O'Driscoll C, Kenna P, Cotter TG. Enhancing survival of photoreceptor cells in vivo using the synthetic progestin Norgestrel. *J Neurochem*. 2011;118:915–927.
25. Byrne AM, Ruiz-Lopez AM, Roche SL, et al. The synthetic progestin norgestrel modulates Nrf2 signaling and acts as an antioxidant in a model of retinal degeneration. *Redox Biol*. 2016;10:128–139.
26. Roche SL, Wyse-Jackson AC, Gomez-Vicente V, et al. Progesterone attenuates microglial-driven retinal degeneration and stimulates protective fractalkine-CX3CR1 signaling. *PLoS One*. 2016;11:e0165197.
27. Wyse Jackson AC, Cotter TG. The synthetic progesterone Norgestrel is neuroprotective in stressed photoreceptor-like cells and retinal explants, mediating its effects via basic fibroblast growth factor, protein kinase A and glycogen synthase kinase 3beta signalling. *Eur J Neurosci*. 2016;43:899–911.
28. Roche SL, Wyse-Jackson AC, Ruiz-Lopez AM, Byrne AM, Cotter TG. Fractalkine-CX3CR1 signaling is critical for progesterone-mediated neuroprotection in the retina. *Sci Rep*. 2017;7:43067.
29. Chang GQ, Hao Y, Wong F. Apoptosis: final common pathway of photoreceptor death in rd, rds, and rhodopsin mutant mice. *Neuron*. 1993;11:595–605.
30. Murakami Y, Ikeda Y, Nakatake S, et al. Necrotic cone photoreceptor cell death in retinitis pigmentosa. *Cell Death Dis*. 2015;6:e2038.
31. Eaton SL, Roche SL, Llavero Hurtado M, et al. Total protein analysis as a reliable loading control for quantitative fluorescent Western blotting. *PLoS One*. 2013;8:e72457.
32. Abdeljalil J, Hamid M, Abdel-Mouttalib O, et al. The optomotor response: a robust first-line visual screening method for mice. *Vis Res*. 2005;45:1439–1446.

Investigative Ophthalmology & Visual Science

33. Mustafi D, Engel AH, Palczewski K. Structure of cone photoreceptors. *Prog Retin Eye Res*. 2009;28:289–302.
34. Roche SL, Ruiz-Lopez AM, Moloney JN, Byrne AM, Cotter TG. Microglial-induced Muller cell gliosis is attenuated by progesterone in a mouse model of retinitis pigmentosa. *Glia*. 2018; 66:295–310.
35. Murakami Y, Yoshida N, Ikeda Y, et al. Relationship between aqueous flare and visual function in retinitis pigmentosa. *Am J Ophthalmol*. 2015;159:958–963.
36. Bringmann A. Cellular signaling and factors involved in Muller cell gliosis: neuroprotective and detrimental effects. *Prog Retin Eye Res*. 2009;28:423–451.
37. Cuenca N, Fernandez-Sanchez L, Campello L, et al. Cellular responses following retinal injuries and therapeutic approaches for neurodegenerative diseases. *Prog Retin Eye Res*. 2014; 43:17–75.
38. Komeima K, Rogers BS, Lu L, Campochiaro PA. Antioxidants reduce cone cell death in a model of retinitis pigmentosa. *Proc Natl Acad Sci U S A*. 2006;103:11300–11305.
39. Usui S, Oveson BC, Lee SY, et al. NADPH oxidase plays a central role in cone cell death in retinitis pigmentosa. *J Neurochem*. 2009;110:1028–1037.
40. Ott M, Gogvadze V, Orrenius S, Zhivotovsky B. Mitochondria, oxidative stress and cell death. *Apoptosis*. 2007;12:913–922.
41. Lin MT, Beal MF. Mitochondrial dysfunction and oxidative stress in neurodegenerative diseases. *Nature*. 2006;443:787.
42. Comitato A, Sanges D, Rossi A, Humphries MM, Marigo V. Activation of Bax in three models of retinitis pigmentosa. *Invest Ophthalmol Vis Sci*. 2014;55:3555–3562.
43. Yin P, Lin Z, Cheng YH, et al. Progesterone receptor regulates Bcl-2 gene expression through direct binding to its promoter region in uterine leiomyoma cells. *J Clin Endocrinol Metab*. 2007;92:4459–4466.
44. Byrne AM, Roche SL, Ruiz-Lopez AM, Jackson AC, Cotter TG. The synthetic progestin norgestrel acts to increase LIF levels in the rd10 mouse model of retinitis pigmentosa. *Mol Vis*. 2016;22:264–274.
45. Ruiz Lopez AM, Roche SL, Wyse Jackson AC, et al. Pro-survival redox signalling in progesterone-mediated retinal neuroprotection. *Eur J Neurosci*. 2017;46:1663–1672.
46. Wyse-Jackson AC, Roche SL, Ruiz-Lopez AM, et al. Progesterone analogue protects stressed photoreceptors via bFGF-mediated calcium influx. *Eur J Neurosci*. 2016;44:3067–3079.
47. McInnes C, Sykes BD. Growth factor receptors: structure, mechanism, and drug discovery. *Biopolymers*. 1997;43:339–366.
48. Leung EY, Kim JE, Askarian-Amiri M, et al. Relationships between signaling pathway usage and sensitivity to a pathway inhibitor: examination of trametinib responses in cultured breast cancer lines. *PLoS One*. 2014;9:e105792.
49. Pettirossi V, Santi A, Imperi E, et al. BRAF inhibitors reverse the unique molecular signature and phenotype of hairy cell leukemia and exert potent antileukemic activity. *Blood*. 2015; 125:1207–1216.
50. Slack C, Alic N, Foley A, et al. The Ras-Erk-ETS-signaling pathway is a drug target for longevity. *Cell*. 2015;162:72–83.
51. Kitai H, Ebi H, Tomida S, et al. Epithelial-to-mesenchymal transition defines feedback activation of receptor tyrosine kinase signaling induced by MEK inhibition in KRAS-mutant lung cancer. *Cancer Discov*. 2016;6:754–769.
52. Carter-Dawson LD, LaVail MM. Rods and cones in the mouse retina. I. Structural analysis using light and electron microscopy. *J Comp Neurol*. 1979;188:245–262.
53. Li Y, Tao W, Luo L, et al. CNTF induces regeneration of cone outer segments in a rat model of retinal degeneration. *PLoS One*. 2010;5:e9495.
54. Loibl S, Gianni L. HER2-positive breast cancer. *Lancet*. 2017; 389:2415–2429.
55. Faivre EJ, Lange CA. Progesterone receptors upregulate Wnt-1 to induce epidermal growth factor receptor transactivation and c-Src-dependent sustained activation of Erk1/2 mitogen-activated protein kinase in breast cancer cells. *Mol Cell Biol*. 2007;27:466–480.
56. Lange CA, Richer JK, Shen T, Horwitz KB. Convergence of progesterone and epidermal growth factor signaling in breast cancer. Potentiation of mitogen-activated protein kinase pathways. *J Biol Chem*. 1998;273:31308–31316.
57. Evans RM. The steroid and thyroid hormone receptor superfamily. *Science*. 1988;240:889–895.
58. Goldman D. Muller glial cell reprogramming and retina regeneration. *Nat Rev Neurosci*. 2014;15:431–442.
59. Karl MO, Hayes S, Nelson BR, et al. Stimulation of neural regeneration in the mouse retina. *Proc Natl Acad Sci U S A*. 2008;105:19508–19513.
60. Ueki Y, Reh TA. EGF stimulates Muller glial proliferation via a BMP-dependent mechanism. *Glia*. 2013;61:778–789.
61. Ooto S, Akagi T, Kageyama R, et al. Potential for neural regeneration after neurotoxic injury in the adult mammalian retina. *Proc Natl Acad Sci U S A*. 2004;101:13654–13659.
62. Close JL, Liu J, Gumuscu B, Reh TA. Epidermal growth factor receptor expression regulates proliferation in the postnatal rat retina. *Glia*. 2006;54:94–104.
63. Wan J, Ramachandran R, Goldman D. HB-EGF is necessary and sufficient for Muller glia dedifferentiation and retina regeneration. *Dev Cell*. 2012;22:334–347.


Investigative Ophthalmology & Visual Science